Active noise control in motorcycle helmets: Feedback, Feedforward, LTI and LPV approaches

Rosa Castañé-Selga† Fernando Bianchi‡ Ricardo S. Sánchez-Peña§

†Lehrstuhl für Regelungstechnik, Technische Universität München, Germany
rosa.castane@tum.de
‡Sistemas Avanzados de Control, Universitat Politècnica de Catalunya, Spain, fernando.bianchi@upc.edu
§CONICET e Instituto Tecnológico de Buenos Aires, Argentina, rsanchez@itba.edu.ar

Abstract— **Recent Noise at Work Regulations in the EU (2003) have been established to prevent Noise Induced Hearing Loss (NIHL). This imposes more demanding performance results as compared to traditional active noise control (ANC) in motorcycle helmets. Usual solutions are presented in terms of linear time invariant (LTI) feedback (FB) controllers, which generally produce poor results. Here an experimental identification of the error microphone-speaker model is used to design a linear parameter varying (LPV) feedback controller. The parameter which schedules the LPV controller is the air velocity, which can be measured in real-time. It was tested against a road test experiment and produced promising results. In order to further increase the noise attenuation, two improvements should be studied: the addition of a feedforward (FF) control to implement an hybrid (FF/FB) solution and the best location of an external noise microphone (used as a FF signal). A discussion on both issues is presented at the end of this paper as an ongoing research issue, which could potentially provide the required attenuation expected from the EU Noise Regulations.**

Keywords— **motorcycle helmet noise, active noise control, robust control, identification, invalidation**

1. INTRODUCTION

ANC in motorcycle helmets has received special attention in the last few years due to the recent European legislation of noise in work environments ([19]). This legislation, establishes a maximum level of noise that workers can suffer during a regular working day ($<$ 87 dB(A)) in order to prevent NIHL. The problem is that is very difficult to comply these laws with existing technology. In particular, occupational motorcyclists such as policemen, delivery employees, sportsmen, are in risk of NIHL. Several medical studies ([20, 10, 9, 7]) point out that, with the inner helmet noise levels and the typical driving patterns, the percentage of exposed population that will suffer a hearing loss of 30 dB or more ranges from 40% for professional racers, 36% for paramedics and 6% for driving instructors.

In 1997 ([8]) the use of noise cancelling earphones in full coverage style helmets was patented and proved that the use of ANC techniques does not present the disadvantages of earplugs or proprietary neck seals. Nevertheless, the traditional ANC used in helmets is based only on feedback, whose limitations have been extensively studied ([17]) and produces low performance in general.

All the works on ANC in helmets are based on a feedback scheme which suffers well known limitations and have in general low performance. Feedforward controllers instead are not subject to the typical performance limitations of the feedback loop, but need to guarantee a stable behavior and its performance is directly related to model uncertainty. Some previous results with this hybrid control configuration can be found in [3]. In addition, the time varying nature of the system may be described as an LPV model, hence a potentially important improvement in performance can be obtained through the use of an hybrid LPV controller ([4]). To the authors knowledge there is no previous result with this structure.

In order to test if the FF approach is useful, a good LTI or LPV model of the external noise signal should be obtained. To this end a reference microphone should be placed in the helmet so that it senses the external noise. In addition, an experiment should be made to acquire the necessary data to identify this model, either LTI or LPV. In the latter case, a scheduling parameter should also be measured, in this case the air velocity.

Here, two experiments have been made. The first one was performed in a laboratory in order to identify the reference–error microphone model and the error microphone–speaker model. The first model could be used in the implementation of a FF control solution, and the second one is used to design a FB controller. In both cases the identification was made by means of an interpolation parametric/non-parametric robust identification method ([13]) which also produced an uncertainty frequency dependent weight. For the error microphone–speaker model used in the FB solution, the augmented plant included a parameter dependent performance weight which provides a better attenuation according to the velocity changes. Hence, the augmented plant is an LPV model scheduled by the air velocity and an LPV controller was designed to control it. The results were promising for different velocity tests and also for a simulated velocity profile using experimental data obtained from the second experi-

Figure 1: Setup for the freeway experiment: mannikin and helmet with microphones and anemometer, all located in the car's roof.

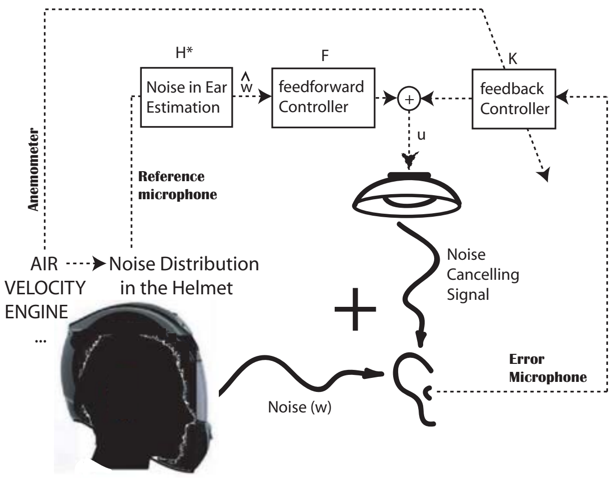

Figure 2: Scheme of the hybrid control configuration and all the sensors and controllers involved in the control design.

ment.

The second experiment was a road test which acquired data from the error microphone, several reference microphones and the air velocity, which ranged from 20 to 120 km/h (26 to 150 km/h of air speed). Here the helmet was mounted on a car's roof and driven in the freeway (see Fig. 1). The objective was twofold: determine I/O data to identify the best model (either LTI or LPV) of the reference–error microphone system, and locate the best position of the reference microphone. The latter is the key in providing the input noise signal to the FF controller.

The paper is organized as follows. Next section provides a brief background on the control structure and the identification and invalidation methods. Section 3presents the FB identification and controller results. Section 4introduces a discussion on FF identification models and sensor location, which could be useful in future hybrid (FF/FB) controller implementations. The paper ends with concluding remarks and future research directions.

2. BACKGROUND

2.1. Control Structure

The three parts of the control structure can be seen in Fig. 2 and 3 :

- **Noise direct path identification:** The noise that affects the ear of the motorcyclist should be predicted and used in the feedforward path. To this end, an identification of the transfer function between the reference and the error microphones should be made.
- **Feedforward Controller:** The noise prediction will be used as the input to the FF controller, which could provide high levels of attenuation as it is not subject to the feedback loop limitations. A FF controller could be designed taking into account the uncertainty introduced by the noise prediction as in [4] using results from [16].
- **Feedback Controller:** The information provided by the feedback (error) microphones will be the input to the FB controller, and in addition the air speed, measured by the anemometer, will modify its dynamics and turn it a feedback LPV controller. Here, the fact that the noise spectrum changes (in magnitude and bandwidth) with the relative velocity $v(t)$ has been used. A velocity varying performance weight $W_{fb}(v)$ modifies the augmented model used in the feedback LPV controller design. This works as a *tuning* of the performance with air speed $v(t)$, therefore producing a better attenuation than if a single time invariant weight $W_{fb}(s)$ were used for all velocity changes. This controller guarantees robust stability and performance of the closed loop.

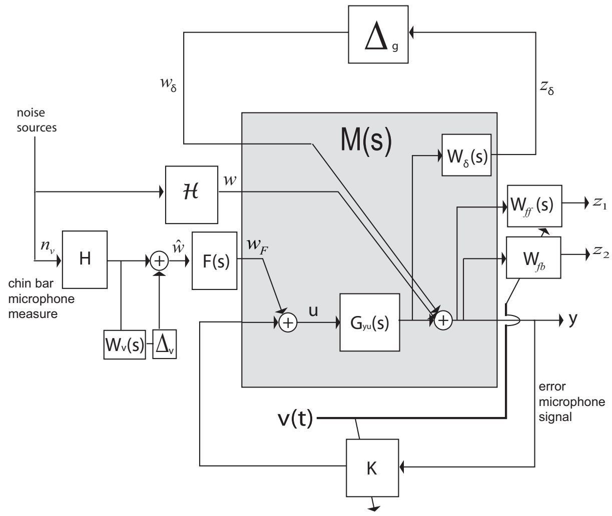

Figure 3: Control configuration with the FB and FF controllers for both, the LTI and LPV cases.

Notice that the way to introduce the noise cancelling signal in both, the FB and FF controllers, is through the speakers (earphones). Hence, their model and level of uncertainty have to be taken into account in the design.

The control structure that could be used in an hybrid (FF/FB) solution to the problem is illustrated by Fig. 3. There are several two-degree-of-freedom structures that could have been chosen as has been studied in a previous work ([3]), the structure presented here provides better possibilities. Let us define as the actual transfer function between the chin bar noise (n_v) and the ear noise (w) as $\mathcal{H}$, and its nominal model as H. The FF controller is represented by $F(s)$ and H and the LPV FB controller as $K[v(t)]$. The uncertainty of the speaker model is represented by Δ_g and the uncertainty in the prediction of the noise in the ear is defined as Δ_v. Note that $W_{ff}(s)$ and $W_{fb}[v(t)]$ are used as performance weights and $W_\delta(s)$ is a robustness weight. $W_v(s)$ can be interpreted as the level of uncertainty in the prediction of the noise in the ear and it works exactly as a performance weight that can be included in W_{ff}. Notice that if no active noise control is used, the actual noise in the ear would be $y = w$. In this work, only the LPV FB solution has been implemented.

2.2. Identification/Invalidation algorithms

The error microphone–speaker model was identified by means of a laboratory experiment described in section 3. The identification procedure is based on a parametric/non-parametric interpolation procedure which has a convex formulation based on LMI (Linear Matrix Inequalities) [13]. It is based on an extension of the Nevanlinna-Pick and Caratheodory-Fejer interpolation theories which includes noisy frequency and time domain data ([14]). In addition, a dynamic multiplicative uncertainty model is assumed and an uncertainty weight $W_\delta(s)$ is computed based on the experimental data and the nominal model. The theoretical background is related to the robust identification area (see [15, 5] and references therein). This procedure is well fitted to determine the low frequency dynamics, but requires more work than a straightforward procedure as subspace identification. It has been used here due to the fact that this model is LTI and only one identification is necessary to design the FB controller.

The candidate models for the reference–error microphone system were computed by means of a subspace identification procedure ([12]) followed by a model invalidation step, in order to determine the uncertainty and noise error bounds. This has been used here due to the fact that a possible LPV candidate model could be obtained, therefore models for all different velocities would have to be identified. Also, the fact that invalidation methods provide a noise energy bound is useful to predict the amount of potential attenuation of the FF solution. Next we present a brief introduction to the invalidation process that has been used, based on [18]. Here, the first attempt is to produce a not-invalid LTI model, followed by an affine LPV model, as investigated in [2].

Consider an LPV system

$$G(\rho) : \begin{cases} x_{k+1} = A(\rho_k)x_k + B(\rho_k)u_k, \\ y_k = C(\rho_k)x_k + D(\rho_k)u_k \end{cases} \qquad (1)$$

where ρ_k is related with the value of the wind velocity in the sample k and the uncertainty and external signal d sets are:

$$\Delta \in \mathbf{\Delta} \stackrel{\triangle}{=} \{\Delta \in \mathcal{H}_\infty : \|\Delta\|_\infty \leq \delta \leq 1\}, \qquad (2)$$

$$d \in \mathcal{D} \stackrel{\triangle}{=} \{d \in \mathbb{R}^r : \|d\|_2 < d_{\max}\} \qquad (3)$$

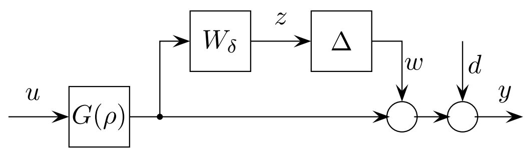

Figure 4: Assumed model uncertainty representation

and the error model setup of Fig. 4.

The following result verifies if the uncertainty model of Fig. 4, the uncertainty (2) and noise (3) sets are consistent with the experimental data ([18]). Here, vectors $\mathbf{d}, \mathbf{y}, \mathbf{u}$ and $\mathbf{w}$ represent their truncated version: $\mathbf{x} = \left[x_o^T \cdots x_{n-1}^T \; x_n^T\right]^T$ and T_x represents the (finite) Toeplitz matrix corresponding to a (truncated) signal $\mathbf{x}$ or the (truncated) impulse response of a linear discrete operator.

Theorem 21 *Given time-domain measurements of the input u, the output y and the time-varying parameter ρ, the LPV model $G(\rho)$ is not invalidated by this experimental information if and only if there exist two vectors d and w, such that*

$$\begin{aligned} &\begin{bmatrix} (T_{G_\Delta}T_u)^T T_{G_\Delta}T_u & T_w^T \\ T_w & \delta^2 I \end{bmatrix} > 0, \\ &\begin{bmatrix} d_{\max}^2 & \mathbf{d}^T \\ \mathbf{d} & I \end{bmatrix} > 0 \\ &\mathbf{d} = \mathbf{y} - T_G\mathbf{u} - \mathbf{w} \end{aligned} \qquad (4)$$

3. FEEDBACK RESULTS

3.1. Identification

The error microphone–speaker model was identified by means of a laboratory experiment, assuming it has an LTI input-output relation. Based on this hypothesis, the system was excited by a multi-sine wave introduced through the speaker, measuring the output data from the error microphone. The microphones are collocated with respect to the speakers and, therefore, the uncertainty due to how the helmet is worn is not considered. The excitation frequency range was from 20 to 1500 Hz with a 5 Hz frequency resolution. Note that the identified system involves not only the electro-mechanical system of the speaker and the microphone, but also how the sound pressure is transmitted between the two devices. This experiment has been carried out for both sides of the helmet and the results are illustrated in Fig. 5. As mentioned previously, the identification is based on a parametric/non-parametric interpolation procedure which has a convex LMI formulation (see [13, 14]).

3.2. Controller Results

Once the transfer functions $G_{o,\ell}(s)$ and $G_{o,r}(s)$ for the left and right respectively, feedback paths of the helmet were obtained (see Fig. 5), their robustness weight $W_\delta(s)$ was computed. The latter should cover the relative uncertainty

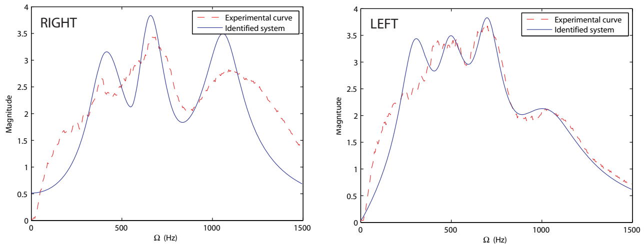

Figure 5: Identification results for left ($G_{o,\ell}$) and right ($G_{o,r}$) microphone–speaker models (used in the FB design).

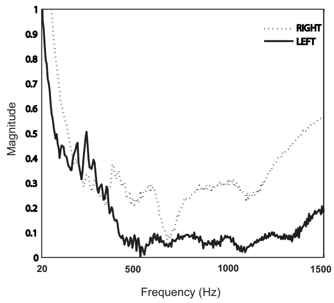

Figure 6: Relative uncertainty for left and right microphone–speaker models, which are covered by $W_\delta(s)$ (used in the FB design).

as follows:

$$|W_\delta(\jmath\omega)| \quad \geq \quad \left|\frac{G(\jmath\omega) - G_{0,i}(\jmath\omega)}{G_{0,i}(\jmath\omega)}\right| \qquad i \in \{\ell, r\}$$

as used in a multiplicative uncertainty structure, i.e. $G = \{G_{o,i}(1 + W_\delta\Delta), \quad |\Delta| < 1\}, i \in \{\ell, r\}$. The relative uncertainty errors in both sides of the helmet are illustrated in Fig. 6, which are very similar.

Due to their similarity and for the sake of simplicity, the robustness weight is the same for both sides of the helmet, and has been chosen to be first order to limit the controller order:

$$W_\delta(s) \quad = \quad 2.7 \times \frac{s + 104}{s + 520}$$

In previous works ([4]) it was observed that the amplitude and the bandwidth of the noise increased with the air velocity around the motorcycle helmet. Therefore, the idea is to design an LPV performance weight that will help in achieving more performance in the bandwidth were the most annoying frequencies are concentrated at each velocity. Then, according to the information presented in Fig. 7 the performance weight will be concentrated in the low frequencies for low velocities and, otherwise, it will cover from 20 to 1500 Hz for higher velocities. The performance weight is defined as an affine combination of the air velocity, as follows:

$$W_p[v(t)] \quad \equiv \quad \left[\begin{array}{c|c} A_0 & B_0 \\ \hline C_0 & D_0 \end{array}\right] + \left[\begin{array}{c|c} A_1 & B_1 \\ \hline C_1 & D_1 \end{array}\right] \times \frac{v}{v_{max}}$$

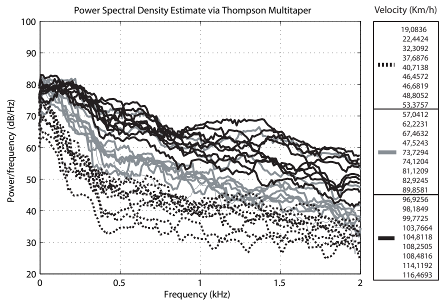

Figure 7: Noise spectra for different values of the car-air velocity in the freeway experiment.

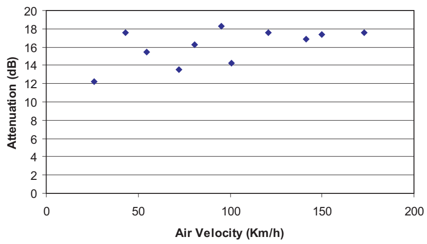

Figure 8: FB controller results for fixed velocities.

The LPV feedback controller is designed using standard procedures ([1, 6]), and the results can be seen in Figs. 8 and 9. In the first figure, the attenuation achieved for fixed velocities using real noise signals obtained in previous experiments ([4]) are presented. Here, the attenuation varies from 12 to 19 dB with a mean of 16 dB. In Fig. 9 the noise attenuation in a 2 min freeway journey is illustrated, and the mean value is similar to the previous one, i.e. 16.3 dB. These results are promising, and encourage the addition of a feedforward controller to achieve the EU regulations. To this end, a discussion on practical implications of a FF implementation are presented in next section.

4. FEEDFORWARD DISCUSSION

4.1. Experimental Setup

With the aim of identifying and evaluating the best input signal for the feedforward controller another experiment was performed. The idea is to symmetrically place a pair of feedforward microphones in different locations of the helmet. This was used to test the efficiency of the location of the reference microphones when used in a FF configuration. Therefore, four feedforward microphones (M1 to M4) were located in the helmet in the positions indicated in Fig. 10 and an error microphone was placed in the ear of the mannikin. The mannikin with the helmet, all reference and error microphones and the anemometer were placed in the roof of a car (Fig. 1). The output voltage for the feedforward and the error microphones were recorded for several values of the air velocity. The objective was twofold, to test the best reference microphone location, and to measure its influence with velocity, in order to identify a reference–error microphone model. Both objectives are related to the

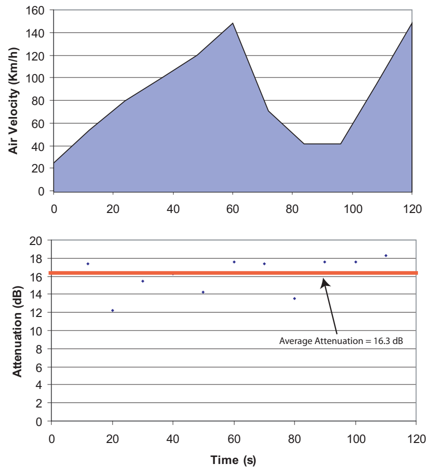

Figure 9: FB controller results for velocity profile.

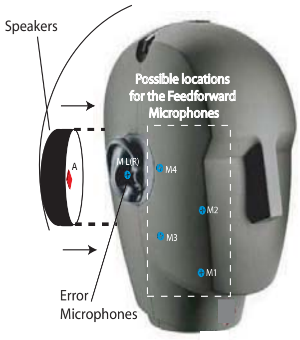

Figure 10: Mannikin used in the experiments: a pair of omnidirectional matched microphones in the ears (error microphones) and several pairs of reference microphones in the chin bars.

use of a FF controller.

4.2. Model Identification and Invalidation

In previous theoretical works, it was concluded that additional noise cancellation can be achieved with the use of a FF control ([4]). In acoustical applications, FB control presents strong performance limitations. These limitations are not present in FF control since stability is not a problem. Therefore, the hybrid (FF/FB) control structure has the potential of improving the performance. However, a central point for the success of this control structure is the need of a good estimation of the surrounding noise, which may be a very difficult task in practice.

In the control configuration scheme of Fig. 3, the estimation of the surrounding noise is equivalent to finding the I/O map H and estimating the modelling errors, i.e., uncertainty and noise bounds. Note that the sizes of the model uncertainty and measurement noise sets impose limits on the improvement achieved by the FF/FB structure with respect to the FB control. In fact, in the typical identification representation, model plus measurement noise, the FF attenuation is directly related to the resulting bound on the measurement noise.

In order to find the model H, first an assumption of an LTI I/O relation between the noise in the reference and error microphones has been made. Based on this hypothesis, the model H was identified in a laboratory experiment. The system was excited by a multi-sine wave generated by a loudspeaker placed in front of the helmet. The sound at the ear and the surrounding sound were sensed with the error and reference microphones, respectively. With this experimental data, H was identified using the parametric/non-parametric interpolation procedure described in [13].

The model obtained from the laboratory data captures the map $\mathcal{H}$ at a $v = 0$ situation. In order to check its validity in real situations, this model was contrasted with data obtained during the freeway experiment. These tests were performed using an invalidation procedure which provides bounds on the model uncertainty and on the measurement noise sets. Due to the fact that this model would be used in a FF scheme, where closed loop stability issues are not of interest, the modelling errors were covered solely by measurement noise. The bounds on this signal and the corresponding worst-case attenuation are listed in Table 1 (second and third columns). Here, high levels of noise and poor attenuation values can be observed. Notice also that the values become worst as the air velocity increases. These results, which are consistent with previous data ([4] and references therein) may be attributed to the increment of the aeroacoustic noise with the air velocity, a phenomenon not present in the laboratory model.

Table 1: RMS values of the measurement noise and its corresponding attenuation

Air velocity	LTI		LPV	
(km/h)	$\|d\|_{\mathrm{rms}}$	Att. (dB)	$\|d\|_{\mathrm{rms}}$	Att. (dB)
25.92	0.26	1.19	0.28	0.52
54.72	3.54	0.46	3.16	1.44
72.00	1.35	0.64	0.89	4.17
100.80	1.82	0.22	2.36	−2.03
120.96	4.81	0.61	4.13	1.94
149.76	4.52	0.66	4.58	0.53

With the purpose of finding a better model for $\mathcal{H}$, we identified an LTI model for each air velocity (to fit an LPV structure) using the freeway experimental data. The noise bounds and the worst-case attenuation are shown in the forth and fifth columns of Table 1. Again, high levels of noise and poor attenuation can be observed. One would expect to find a better model in this case since the actual experimental data was used. However, the values in Table 1 reveals a poor fitting between the models and the data. This fact can only be attributed to the lack of correlation between the noise in the error microphone and in the reference microphone.

This inconsistency between the models and the freeway experimental data reveals the serious difficulties to find pre-calculated models. This is a consequence of the complex aeroacoustics phenomena that cannot be included in simple models. A possible direction of research would be to separate the model which comes from the external noise, that may include turbulence, from the one produced by the helmet vibration, which could possibly be measured by an accelerometer. These two models could be identified separately in order to isolate the complex phenomena and be used as input signals to a FF solution. In addition, the same model structure could be used with adaptive algorithms, e.g. NLMS, projection, σ–modified filters, although stability problems ([11]) could arise in this case.

4.3. Sensor location

The results in Table 1 were obtained from data sensed in the M3 location. After repeating the previous identification/validation procedure at all other microphone locations, it was concluded that the best ones are M3 or M4. That is, the estimation of the surrounding noise improves when the reference microphone is closer to the error sensor. The better attenuation values in the case of the M3 microphone are due to the noise sensed in this location is less affected by the turbulence phenomena. However, these are preliminary results that should be confirmed when better models are available.

5. CONCLUSIONS AND FUTURE RESEARCH

Here an LPV feedback controller for ANC in motorcycle helmets has been presented. The results are promising, with attenuations in the order of 16 dB using experimental data obtained from a freeway test.

The possibility of implementing an hybrid solution by the addition of a FF controller is still to be determined. The best location of a reference microphone to be used as an input signal for a FF scheme was studied, also using experimental data from the road test. In addition, different attempts to determine a good model, either LTI or LPV, for the reference–error microphone path were made. The results are still preliminary, and a deeper understanding of the physical phenomena involved needs to be made in this case.

6. ACKNOWLEDGMENTS

This work was supported in part by the Research Commission of the *Generalitat de Catalunya* (ref. 2005SGR00537), and by the Spanish CICYT DPI2008-00403. The second and third authors would like to acknowledge the support of MEC (Spain) and the PRH Progam of MinCyT (Argentina), respectively. All authors gratefully acknowledge the contribution at UPC of the Dept. of Electronics (Terrassa) for their collaboration in the road experience, and to Epicurus (341-270 BCE).

REFERENCES

[1] Gregory Scott Becker and Andy Packard. Robust performance of LPV systems using parametrically-dependent linear feedback. *Systems and Control Letters*, 23:205–215, 1994.

[2] F. Bianchi and R.S. Sánchez Peña. Robust identification/invalidation in an LPV framework. *International Journal of Robust and Nonlinear Control*, DOI: 10.1002/rnc.1430, 2009.

[3] R. Castañé and R.S. Sánchez Peña. Control activo de ruido acústico en cascos de motociclismo. *Revista Iberoamericana de Automática e Informática Industrial*, 4(3):73–85, 2007.

[4] R. Castañé and R.S. Sánchez Peña. Active Noise Hybrid Time-varying Control for Motorcycle Helmets. to appear in IEEE Transactions on Control System Technology DOI 10.1109/TCST.2009.2025187, 2009.

[5] Jie Chen and Guoxiang Gu. *Control-Oriented System Identification - An $\mathcal{H}_\infty$ Approach*. Willey Inter-Science, 2000.

[6] Pascal Gahinet and Pierre Apkarian. A convex characterization of gain-scheduled $\mathcal{H}_\infty$ controllers. *IEEE Transactions on Automatic Control*, 40(5):853–864, May 1995.

[7] Chris Jordan. Noise induced hearing loss in occupational motorcyclists. *Journal of Enviromental Health Research*, 3:373–382, 2004.

[8] John J. Lazzeroni and Melinda K. Carevich. Noise cancelling microphone for full coverage style helmets. *U.S Patent Office*, 1997.

[9] Andrew W. McCombe. Hearing loss in motorcyclists: occupational and medicolegal aspects. *Journal of the Royal Society of Medicine*, 96:7–9, 2003.

[10] Andrew W. McCombe, J. Binnington, and D. Nash. Two solutions to the problem of noise exposure for motorcyclists. *Occupational Medicine*, 44:239–242, 1994.

[11] R. Ortega and Yu Tang. Robustness of adaptive controllers-a survey. *Automatica*, 25(5):651–77, 1989.

[12] P. Van Overschee and B. De Moor. *Subspace Identification for Linear Systems; Theory, Implementation, Applications*. Kluwer Academic Publishers, Dordrecht, The Netherlands, 1996.

[13] Pablo A. Parrilo, Ricardo S. Sánchez Peña, and Mario Sznaier. A parametric extension of mixed time/frequency robust identification. *IEEE Transactions on Automatic Control*, 44(2):364–369, 1999.

[14] Pablo A. Parrilo, Mario Sznaier, Ricardo S. Sánchez Peña, and Tamer Inanc. Mixed time/frequency-domain based robust identification. *Automatica*, 34(11):1375–1389, 1998.

[15] R. S. Sánchez Peña and M. Sznaier. *Robust Systems Theory and Applications*. John Wiley & Sons, Inc., 1998.

[16] G. Scorletti and V. Fromion. Further results on the design of robust $\mathcal{H}_\infty$ feedforward controllers and filters. In *2006 Conference on Decision and Control*, 2006.

[17] M.M. Seron, J.H. Braslavsky, and G.C. Goodwin. *Fundamental Limitations in Filtering and Control*. Springer, 1997.

[18] Mario Sznaier and María C. Mazzaro. An LMI approach to control-oriented identification and model (in)validation of LPV systems. *IEEE Transactions on Automatic Control*, 48(9):1619–1624, 2003.

[19] UE-2003/10/EC. *Directive 2003/10/EC, Noise at Work Regulations*. Official Journal of the European Community, 2003.

[20] Magleby TD Torian GE. Van Moorhem WK, Sheperd KP. The effects of motorcycle helmets on hearing and the detection of warning signals. *Journal of Sound and Vibration*, 8:30–2, 1981.